scientific reports

Check for updates

OPEN

Adjuvant potential of *Peyssonnelia caulifera* extract on the efficacy of an influenza vaccine in a murine model

Thi Len Ho[1], So Yeon Ahn[2] & Eun-Ju Ko[1,2,3]✉

Natural adjuvants have recently garnered interest in the field of vaccinology as their immunostimulatory effects. In this study, we aimed to investigate the potential use of *Peyssonnelia caulifera* (PC), a marine alga, as a natural adjuvant for an inactivated split A/Puerto Rico/8/1934 H1N1 influenza vaccine (sPR8) in a murine model. We administered PC-adjuvanted vaccines to a murine model via intramuscular prime and boost vaccinations, and subsequently analyzed the induced immunological responses, particularly the production of antigen-specific IgG1 and IgG2a antibodies, memory T and B cell responses, and the protective efficacy against a lethal viral infection. PC extract significantly bolstered the vaccine efficacy, demonstrating balanced Th1/Th2 responses, increased memory T and B cell activities, and improved protection against viral infection. Notably, within 3 days post-vaccination, the PC adjuvant stimulated activation markers on dendritic cells (DCs) and macrophages at the inguinal lymph nodes (ILN), emphasizing its immunostimulatory capabilities. Furthermore, the safety profile of PC was confirmed, showing minimal local inflammation and no significant adverse effects post-vaccination. These findings contribute to our understanding of the immunomodulatory properties of natural adjuvants and suggest the promising roles of natural adjuvants in the development of more effective vaccines for infectious diseases.

Keywords *Peyssonnelia caulifera* (PC), Adjuvant, Influenza vaccine, Th1/Th2 response

Influenza viruses, known to induce annual epidemics and occasional pandemics, pose considerable challenges to public health owing to their significant morbidity and mortality worldwide[1,2]. These viruses predominantly affect respiratory epithelial cells, leading to symptoms varying from mild, such as fever, cough, and malaise, to severe that lead to pneumonia, secondary bacterial infections, and even death in vulnerable groups[3]. Vaccination is the most effective preventive measure against influenza virus infection; however, the rapid antigenic drift and shift of these viruses can compromise the efficacy of vaccines[4,5]. This necessitates the continual development of innovative vaccination strategies and discovery of new antiviral drugs.

The use of potent adjuvants significantly enhances the efficacy of influenza vaccines[6]. Several adjuvants have been approved by the FDA for use in human vaccines, including aluminum salts (alum), monophosphoryl lipid A (MPL), AS01B, CpG1018, Matrix-M, and MF59 [7,8]. Alum has a long history of enhancing antibody responses by activating humoral immunity[9,10]. On the other hand, MPL, which stimulates the toll-like receptor 4 (TLR4) signaling pathway, is used alongside alum in some GlaxoSmithKline vaccines to improve antibody production[11]. The supplementary use of a suitable adjuvant in a vaccine regimen is crucial because it can induce the desired type of immune response and provide optimal protection against diverse infections. An ideal adjuvant, which is integral to the successful immunization of individuals, should stimulate suitable Th1 or Th2 responses[12] and demonstrate high safety, stability, biodegradability, and biocompatibility[13,14]. A delicate balance between Th1/Th2 is often required to provide effective protection against disease, which should be supported by an ideal adjuvant[15,16]. Hence, discovering and developing a new adjuvant that not only enhances the effectiveness of the influenza vaccine but is also safer, more powerful, and cost-effective represents a significant step forward in vaccination technology.

[1]Interdisciplinary Graduate Program in Advanced Convergence Technology & Science, Jeju National University, Jeju 63243, Republic of Korea. [2]Department of Veterinary Medicine, College of Veterinary Medicine, Jeju National University, Jeju 63243, Republic of Korea. [3]Veterinary Medical Research Institute, Jeju National University, Jeju 63243, Republic of Korea. ✉email: eunju@jejunu.ac.kr

One promising area of research that has been gaining attention in the field of vaccine immunology is the use of natural substances as vaccine adjuvants. One subsequent standout is marine algae, with more than one million species on Earth, which have become a focal point of interest[17]. Marine algae, known for their rich and biodiverse metabolic products[18], have surfaced as potential sources of novel adjuvants[19], as they produce various bioactive compounds, including polysaccharides, lipids, and proteins, which have demonstrated potential immunostimulatory properties[20]. In recent years, extracts from specific algae species have been found to evoke considerable immune responses when used as adjuvants[21–23], augmenting both humoral and cell-mediated immune reactions[24]. Therefore, the utilization of algae extract as a natural and potentially more effective adjuvant could represent a significant step forward in improving vaccine efficiency.

We have shown that the extract from *Peyssonnelia caulifera* (PC), a marine algae species, shows immunostimulatory effects on antigen-presenting cell activation in vitro[25]. We, therefore, aimed to assess the effect of PC as an adjuvant in influenza vaccines to boost the immune response, investigate the immunostimulatory effects of PC on the seasonal influenza vaccine, and present evidence of enhanced humoral and cellular responses in mice following intramuscular injection of the PC-adjuvant vaccine. These findings provide a crucial foundation for the development of a superior influenza vaccine adjuvant against seasonal and pandemic influenza.

Results

Effects of PC on antigen-specific antibody production by immunization

To determine whether PC could enhance IgG antibody responses in sera after vaccination, we vaccinated mice and collected immune sera 14 days post-vaccination. Alum was used as a positive adjuvant control. Antigen-specific IgG responses and antibody subtypes in all serum samples were determined by ELISA. Two weeks after prime vaccination, the alum group displayed the highest IgG and IgG1 levels, and PC-induced IgG production was significantly increased compared to that in the sPR8 group. We observed that the PC group exhibited significantly higher IgG2a levels compared to the sPR8 group at a 1:100 dilution (Fig. 1a). Interestingly, consistent with the trend observed in IgG levels following the prime vaccination, the addition of PC resulted in significantly elevated IgG2a antibody levels compared to both the sPR8 and alum groups two weeks after the boost vaccination (Fig. 1b).The data showed PC could enhance Th1 immune responses. All the immunized sera post boost vaccination exhibited protective efficacy against 1×LD50 of A/PR8 (Supplementary Fig. 1).

Effects of PC on antigen-specific T cell responses induced by vaccination

Next, we assessed the effects of PC on T cell proliferation in the lungs and spleen 7 days after the booster vaccination to explore whether PC could stimulate cellular immunity. Lung and spleen cells were harvested, stained with CFSE (carboxyfluorescein succinimidyl ester), cultured in vitro with antigen stimulation for 5

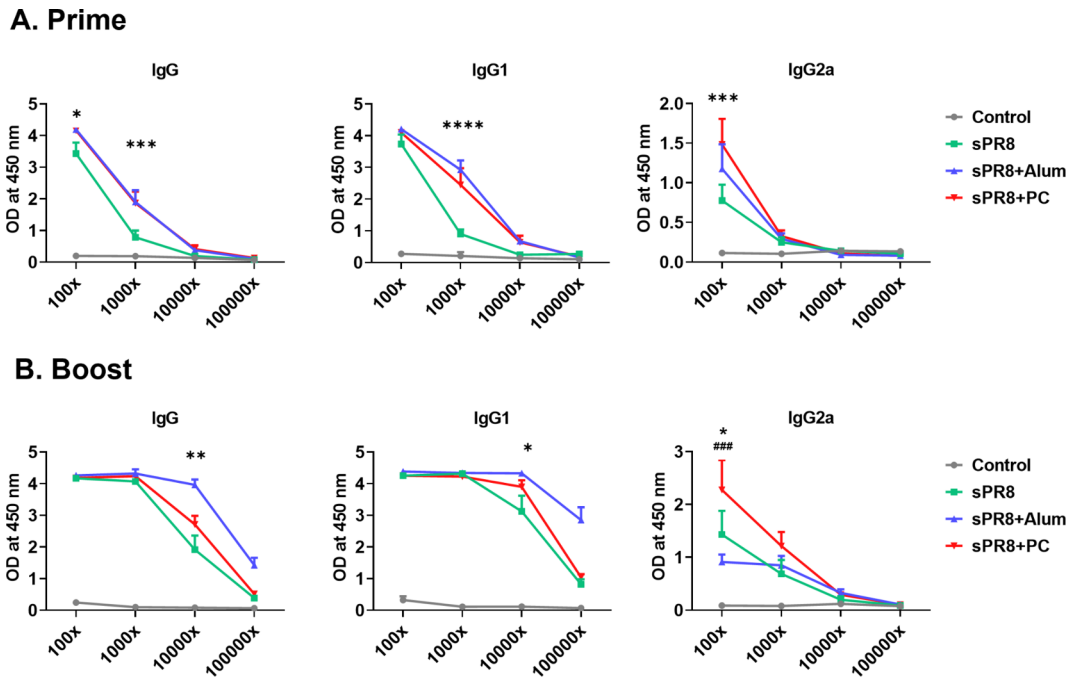

Fig. 1. Antigen-specific antibody levels in sera after immunizations. Mice ($n=4$) were immunized with sPR8 vaccine only or sPR8 in the presence of adjuvants (Alum or PC). Immune sera were taken 2 weeks post prime (**a**) and boost (**b**) immunizations and A/PR8 virus antigen-specific IgG antibody levels were measured by ELISA. Means ± standard errors were shown with individual dots. Two-way analysis of variance (ANOVA) and Tukey's multiple comparison test were performed for statistical analysis. $^{*}p<0.0332$; $^{**}p<0.0021$; $^{***}p<0.0002$, $^{****}p<0.0001$ PC compared to sPR8 group. $\#\#\#p<0.0002$ PC compared to Alum group.

days, and subsequently analyzed using FACS (Fluorescence-activated Cell Sorting). The PC-adjuvant group demonstrated the highest proliferation rates of $CD4^+$ and $CD8^+$ T cells from the lungs, and a significant difference was observed between the PC and alum groups in the lung cell proliferation (Fig. 2a). Vaccination without an adjuvant slightly increased the levels of $CD4^+$ and $CD8^+$ T cell antigen-specific proliferation. Spleen $CD4^+$ T and $CD8^+$ cell proliferation was highest in the PC-adjuvant group (Fig. 2b). The alum group showed slightly increased $CD4^+$ and $CD8^+$ T cell proliferation. Taken together, the PC-adjuvant vaccine significantly increased the antigen-specific proliferation of $CD4^+$ and $CD8^+$ T cells from both the lungs and spleen compared to that in the vaccine-only and alum groups. Overall, PC acts as a potent inducer of T cell activation.

Effect of PC on improving protective efficacy of influenza vaccines after lethal virus infection

Following viral infection, the naïve infection group suffered from a rapid loss of weight, peaking at a 24.17% decrease at 7 days post-infection (Fig. 3a, b). Additionally, only a 50% survival rate was observed on the seventh day post-infection (Fig. 3c). Conversely, all vaccinated groups prevented weight loss and showed markedly superior protective efficiency. Specifically, 7 days after the viral challenge, the PC-adjuvant group significantly bolstered protection against the PR8 virus, evidenced by a minimal body weight loss of just 2.14% and a 100% survival rate. This group outperformed both the alum group, which suffered a 4% body weight loss but maintained a 100% survival rate, and sPR8 group, which endured a 17.36% body weight loss and a 100% survival rate.

Furthermore, we conducted histological examinations of the lungs at 7 days post A/PR8 challenge. The naïve group exhibited severe inflammation, marked tissue damage, and intense infiltration of inflammatory cells. In contrast, the PC group showed reduced immune cell infiltration and inflammation compared to naïve infection group (Fig. 3e). In line with the histological findings, the groups immunized with different vaccines demonstrated a significant reduction in lung viral titers (Fig. 3d).

Effects of PC on lung inflammation after a lethal A/PR8 influenza virus infection

Sixteen weeks after the booster vaccination, the mice were challenged with a lethal dose of the virus. Lung samples were collected 7 days post-infection. Lung cells were used for flow cytometry analysis, and lung supernatant was used for cytokine measurement using ELISA. The highest populations of monocytes, neutrophils, and DCs were observed in the naïve infected group after viral infection (Fig. 4a). The PC-adjuvant group showed a significantly decreased percentage of monocytes and DCs, matching the rate observed in the alum-adjuvant group. However, it presented higher levels of neutrophils than the alum-adjuvant group. A significantly enhanced number of eosinophils was detected in the lungs of the alum-adjuvant group. Both the PC-adjuvant and sPR8 groups showed a moderate population of eosinophils. No significant eosinophil recruitment was observed in the naïve infection group.

The cytokines TNF-α, IL-1β, IL-6, IL-12p40, IFN-γ, and CCL2 were specifically chosen for measurement due to their critical roles in the immune response and inflammatory processes during influenza infection [26,27]. Elevated levels of these cytokines are directly associated with increased lung pathology and have been linked to poor outcomes, including death, in severe cases of influenza [28,29]. Therefore, their measurement provides essential insights into the inflammatory processes and enables us to evaluate the effectiveness and safety of different vaccine strategies in modulating this response. We next measured the expression of tumor necrosis factor-alpha (TNF-α), Interleukin 1 beta (IL-1β), IL-6, IL-12p40, interferon-alpha (IFN-γ), and CCL2 in the lungs. Figure 4b shows that naïve infected mice exhibited the highest levels of all measured cytokines and chemokines (including TNF-α, IL-1β, IL-6, IL-12p40, IFN-γ, and CCL2) following virus infection. These elevated levels indicate robust inflammatory reactions in the lungs against the virus, which are detrimental and not desirable in the context of vaccine-induced immunity. Conversely, vaccinated mice demonstrated a reduction in these inflammatory cytokine levels indicating better protection against the virus. Among these, the PC-adjuvant group showed a significant decrease in IL-1β, IL-6, IFN-γ, IL-12p40, and CCL2 production compared to the naïve infected group. Additionally, the levels of IL-1β, IL-6, IL-12p40, and CCL2 were lower in the PC-adjuvant group compared to the Alum group.

Overall, these results indicated that PC supplemented vaccination significantly reduced the inflammatory reaction against the influenza virus challenge in the lungs, as evidenced by significantly decreased infiltration of inflammatory cells and lower levels of inflammatory cytokines.

Effects of PC on memory T and B cell responses

Memory T and B cells play pivotal roles in the immune response against the influenza virus[30]. Using FACS, we analyzed the presence of antigen-specific memory $CD4^+$ and $CD8^+$ T cells in the lungs and spleen 7 days after a lethal virus challenge. The group vaccinated with PC adjuvant significantly prompted antigen-specific T cell proliferation in the lungs following in vitro stimulation, in both $CD4^+$ and $CD8^+$T cells population (Fig. 5a). In the spleen, the PC-adjuvant vaccine resulted in the highest population of antigen-specific $CD8^+$ memory T cells. The alum group induced a moderate level of $CD8^+$T cell proliferation and showed the highest $CD4^+$T cell in the spleen.

Additionally, PC-adjuvant group generated significantly higher levels of antibody-producing cells in the bone marrow and spleen than the other groups. The alum-adjuvant group exerted a moderate effect on IgG antibody production originating from bone marrow cells, whereas the sPR8 group triggered higher antibody concentrations in spleen cells than the alum group. These findings suggest that the PC adjuvant can effectively stimulate responses from memory T, memory B, and antibody-producing cells.

Effect of PC on DCs and macrophages maturation in vivo

Activation of DCs and macrophages is important to initiate immune responses and immunoregulation[31,32]. We investigated the effect of the PC adjuvant on DC and macrophage maturation at the site of injection and

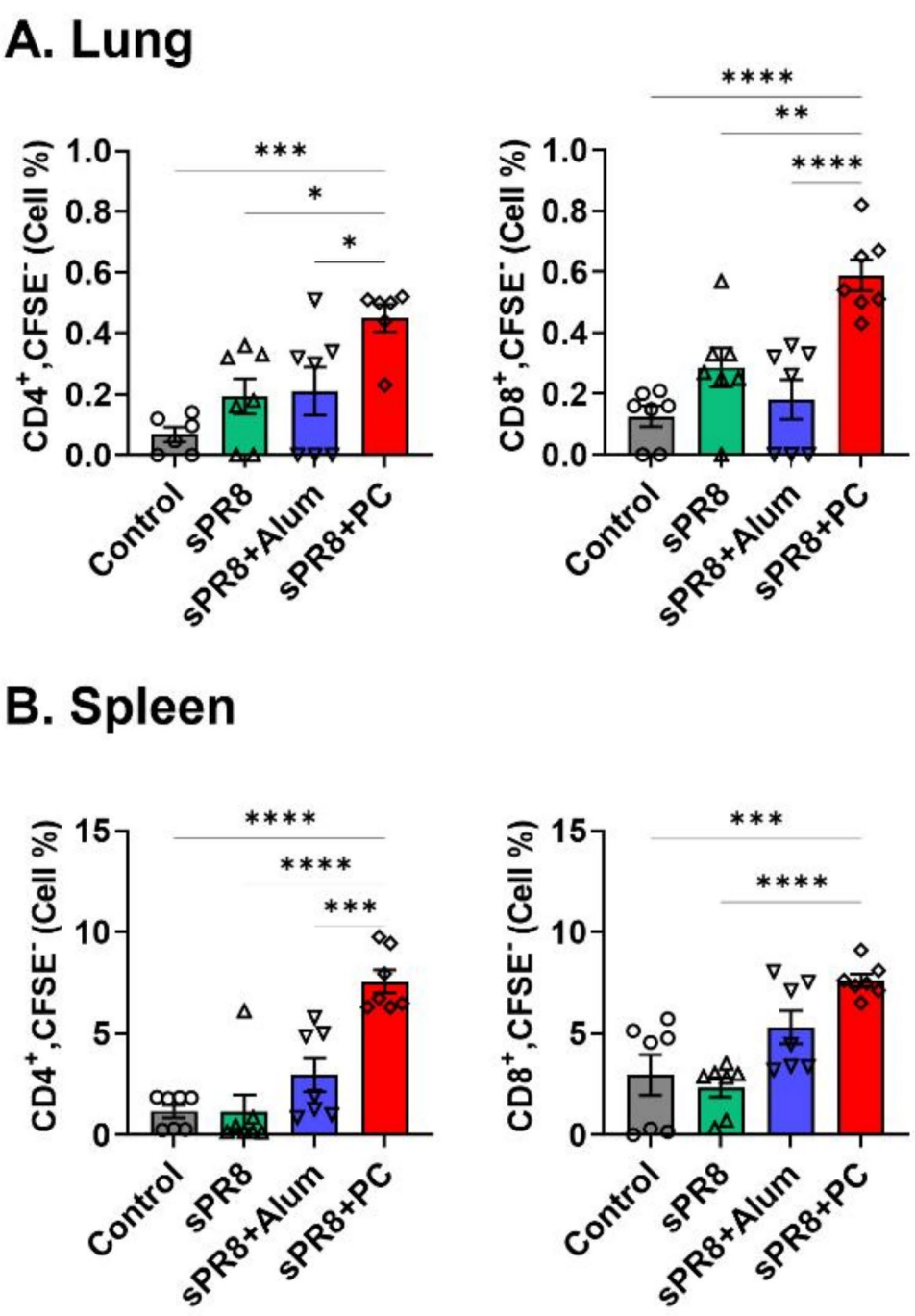

Fig. 2. Antigen-specific T cell responses induced by vaccination. Lung (**a**) and spleen (**b**) cells were harvested from the immunized mice 2 weeks post-boost immunization. CFSE-labeled cells were stimulated with 10 μg/ml sPR8 for 5 days and T cell proliferation was determined by flow cytometry. Means ± standard error are shown with individual dots. One-way ANOVA and Tukey's multiple comparison test were performed for statistical analysis. $^{*}p < 0.0332$; $^{**}p < 0.0021$; $^{***}p < 0.0002$; $^{****}p < 0.0001$ compared between the indicated groups.

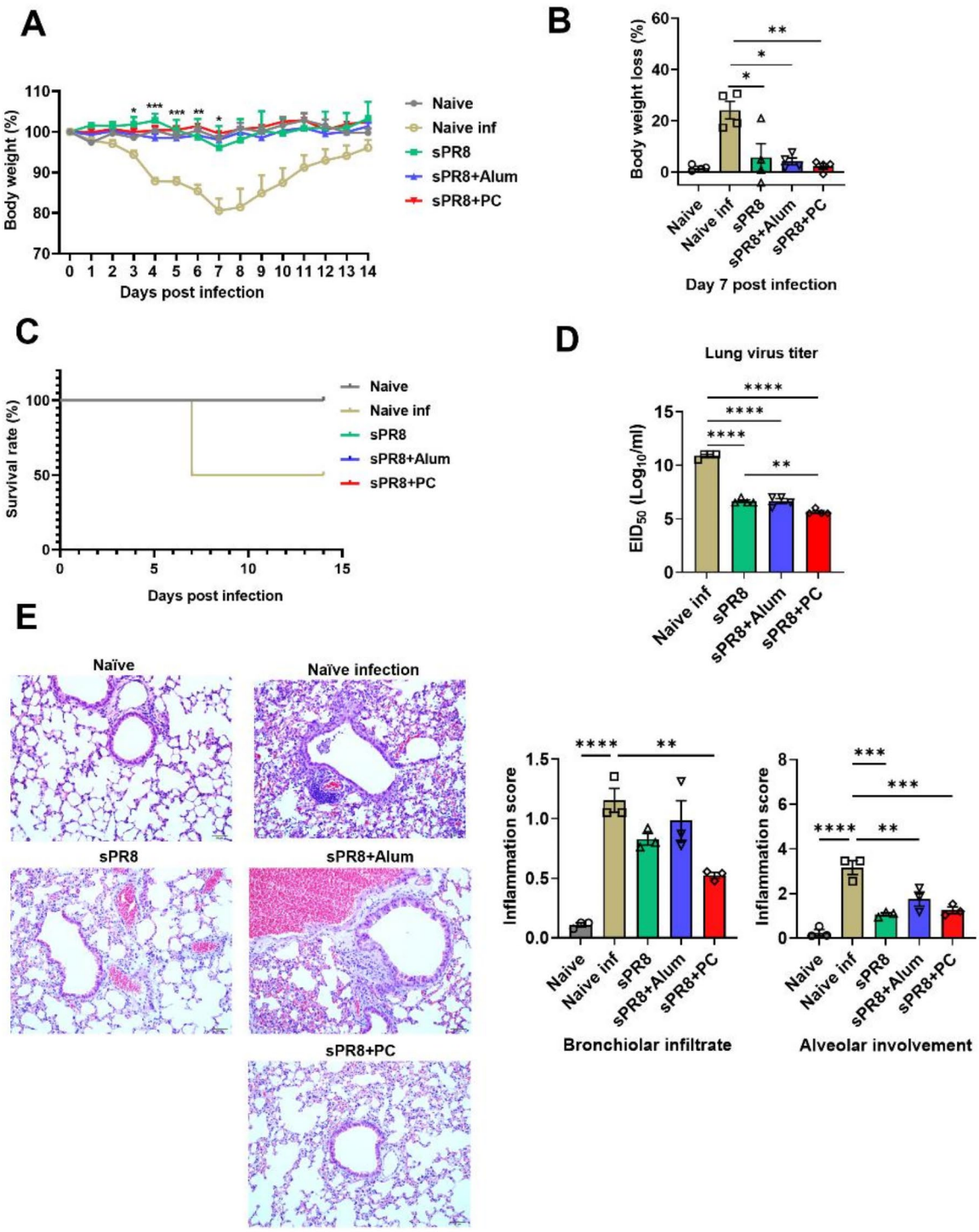

Fig. 3. Protective efficacy of vaccination against a lethal influenza infection. Sixteen weeks after the boost immunization, naïve and immunized mice were infected with a lethal dose of A/PR8 virus (1 × LD50). Sixteen weeks after the booster immunization, naïve and immunized mice were infected with a lethal dose of the A/PR8 virus (1 × LD50). Body weight (**a**) was monitored for 14 days after infection. Body weight loss on day 7 post-infection (**b**), survival rates over 14 days (**c**), viral titration in lung samples harvested 7 days post-infection (**d**), and lung histopathology using hematoxylin and eosin staining (**e**) were assessed. Means ± standard errors were shown with individual dots. One-way ANOVA and Tukey's multiple comparison test were performed for statistical analysis. $^{*}p < 0.0332$; $^{**}p < 0.0021$; $^{***}p < 0.0002$; $^{****}p < 0.0001$ compared between the indicated groups.

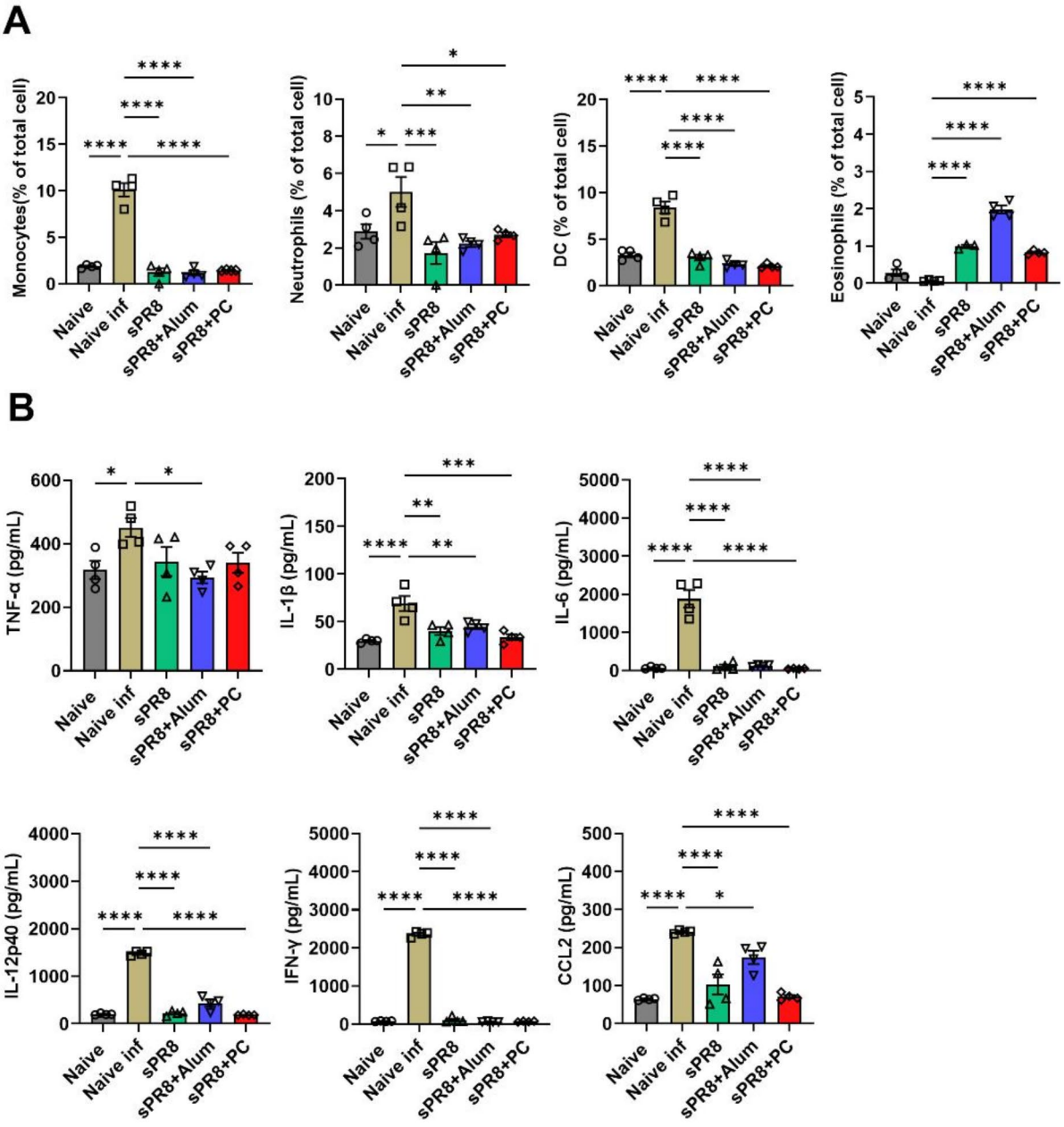

Fig. 4. Cellular infiltration and cytokine production in the lungs after the lethal virus challenge. The immunized mice ($n=4$) were infected with A/PR8 virus (1 x LD50) after 16 weeks of boost immunization. Lung samples were harvested at 7 days post-infection and cell phenotypes were determined by flow cytometry and cytokine levels of each sample were measured by ELISA. Means ± standard errors were shown with individual dots. One-way ANOVA and Tukey's multiple comparison test were performed for statistical analysis. $^{*}p<0.0332$; $^{**}p<0.0021$; $^{***}p<0.0002$; $^{****}p<0.0001$ compared to naïve infected group.

draining lymph nodes. The mice were administered the sPR8 vaccine alone or in combination with either PC or Monophosphoryl lipid A (MPL) via prime and boost immunization. Three days after the booster vaccination, we harvested cells from the injection area, including the muscle tissue and inguinal lymph node (ILN). These cells were then stained for activation markers of DCs and macrophages.

In muscle cells (Fig. 6a, b), MPL vaccination resulted in the highest levels of CD40, CD86, and MHC II in DCs and macrophages. The PC-adjuvant group showed higher levels of MHC II^{high} than the other groups. In contrast, in the ILN (Fig. 6c, d), we observed a significant increase in the expression of all surface molecules

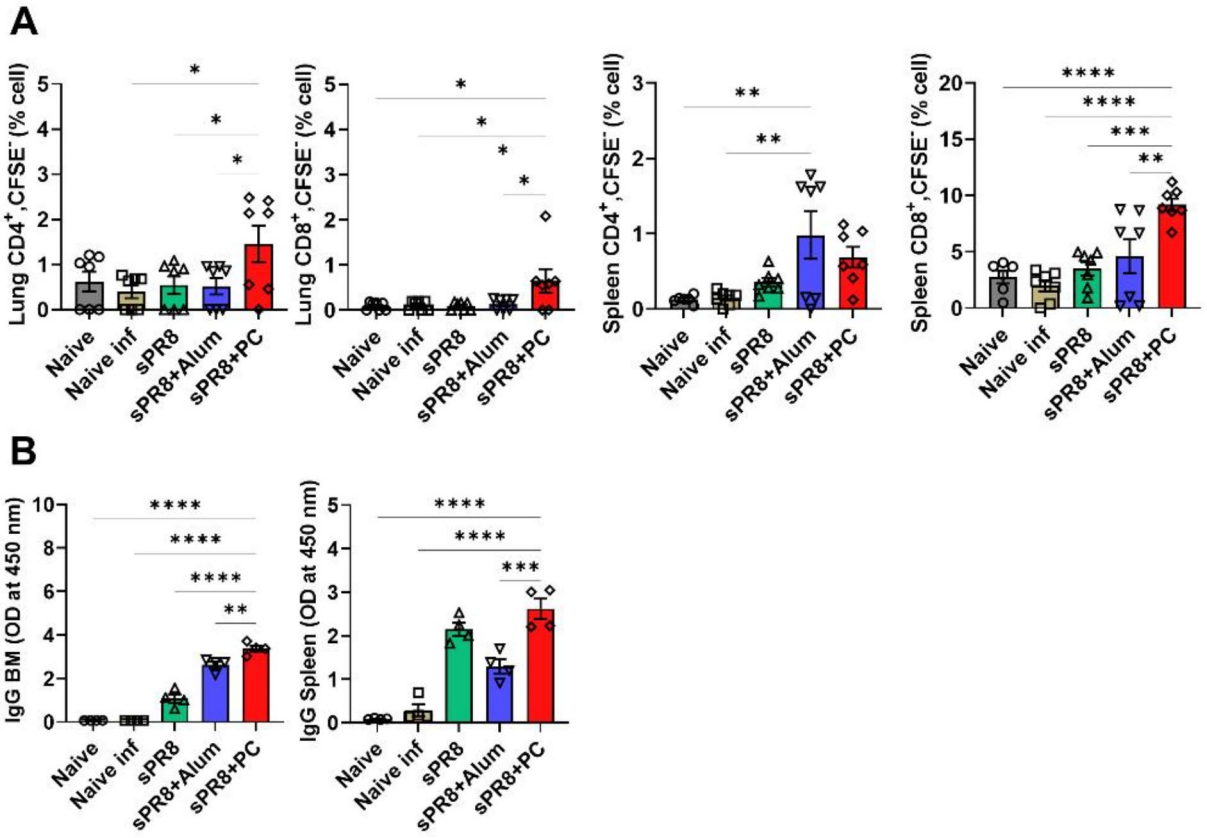

Fig. 5. Antigen-specific memory T and B cell responses induced by the vaccination. Lung, spleen, and bone marrow cells were harvested at day 7 post-infection from the immunized and infected mice. Lung and spleen cells were labeled with CFSE and cultured for 5 days in the presence of sPR8 (10 μg/ml) stimulation. T cell proliferation was then determined via flow cytometry (**a**). Bone marrow cells and spleen cells were also harvested, then incubated with sPR8 (10 μg/ml) for 1 day and 7 days, respectively. Subsequently, antigen-specific IgG production was measured by ELISA (**b**). Means ± standard errors were shown with individual dots. One-way ANOVA and Tukey's multiple comparison test were performed for statistical analysis. $^{*}p < 0.0332$; $^{**}p < 0.0021$; $^{***}p < 0.0002$; $^{****}p < 0.0001$ compared between the indicated groups.

on DCs and macrophages from PC-immunized mice, indicating that PC could stimulate DC and macrophage maturation in vivo effectively.

Furthermore, 3 days after the boost vaccination, we isolated DCs from the spleen and co-cultured them with CFSE-labeled naïve lymphocytes (from C57BL/6 mice) to investigate the antigen presentation and activation ability of the stimulated DCs towards T cells. After 5 days of incubation, T cell proliferation was measured using flow cytometry. The PC-adjuvant group showed a significant increase in the percentage of $CD4^+$ T cell proliferation compared to the other groups (Fig. 6e). $CD8^+$ T cells were induced by PC vaccination but showed lower levels than those in the MPL-adjuvant and sPR8 groups. These data revealed that the PC-adjuvant group effectively promoted DC-induced T cell proliferation.

Effect of PC on local inflammation responses at the injection site

To better understand the local inflammatory response associated with vaccine injection, we performed a muscle histology examination. Mice ($n = 3$) were intramuscularly injected with different vaccine formulations including sPR8 vaccine (0.5 μg/mouse) alone or combined with either PC (200 μg/mouse) or alum (100 μg/mouse) via prime and boost immunizations. Three days after the boost vaccination, muscle tissues were harvested from the injection sites and stained with hematoxylin and eosin (H&E). As shown in Fig. 7, the alum-adjuvant group induced a more severe inflammatory response than the sPR8- and PC-adjuvant groups at 3 days post-boost vaccination. Moderate levels of inflammatory cell infiltration were observed in the muscles of the PC-adjuvant group.

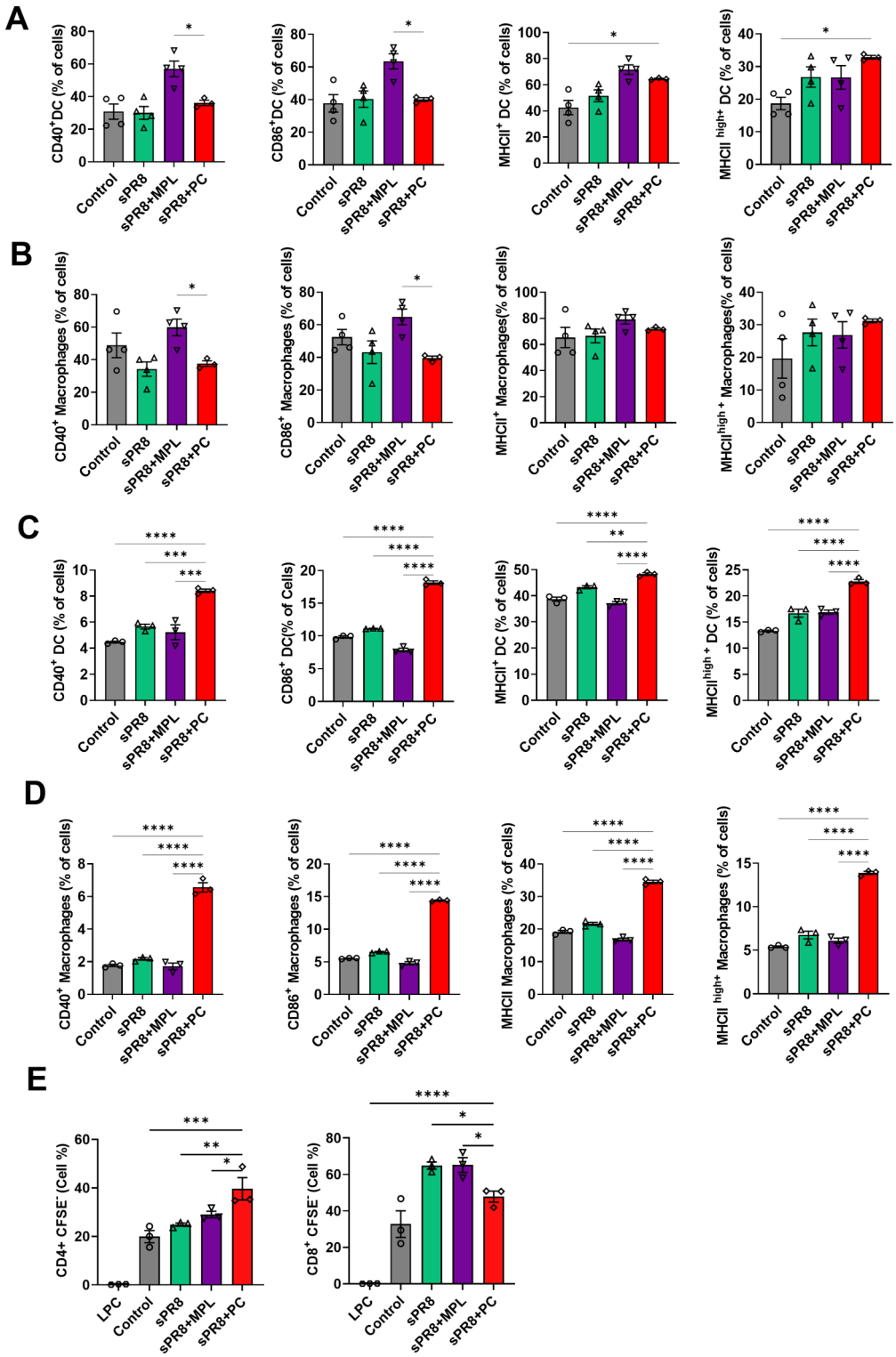

Fig. 6. Activation marker expressions in DCs and macrophages at the site of injection after vaccination. Mice were vaccinated with sPR8 vaccine alone or adjuvanted (PC, MPL). Muscles (**a**, **b**) and ILN (**c**, **d**) samples were harvested at 3 days post-boost vaccination and the activation marker expressions on DCs and macrophages were acquired by flow cytometry. DCs and macrophages were gated by CD11c and CD11b surface markers, respectively. Means ± standard errors are shown with individual dots. One-way ANOVA and Tukey's multiple comparison test were performed for statistical analysis. $^{*}p < 0.0332$; $^{**}p < 0.0021$; $^{***}p < 0.0002$; $^{****}p < 0.0001$ compared to between the indicated groups.

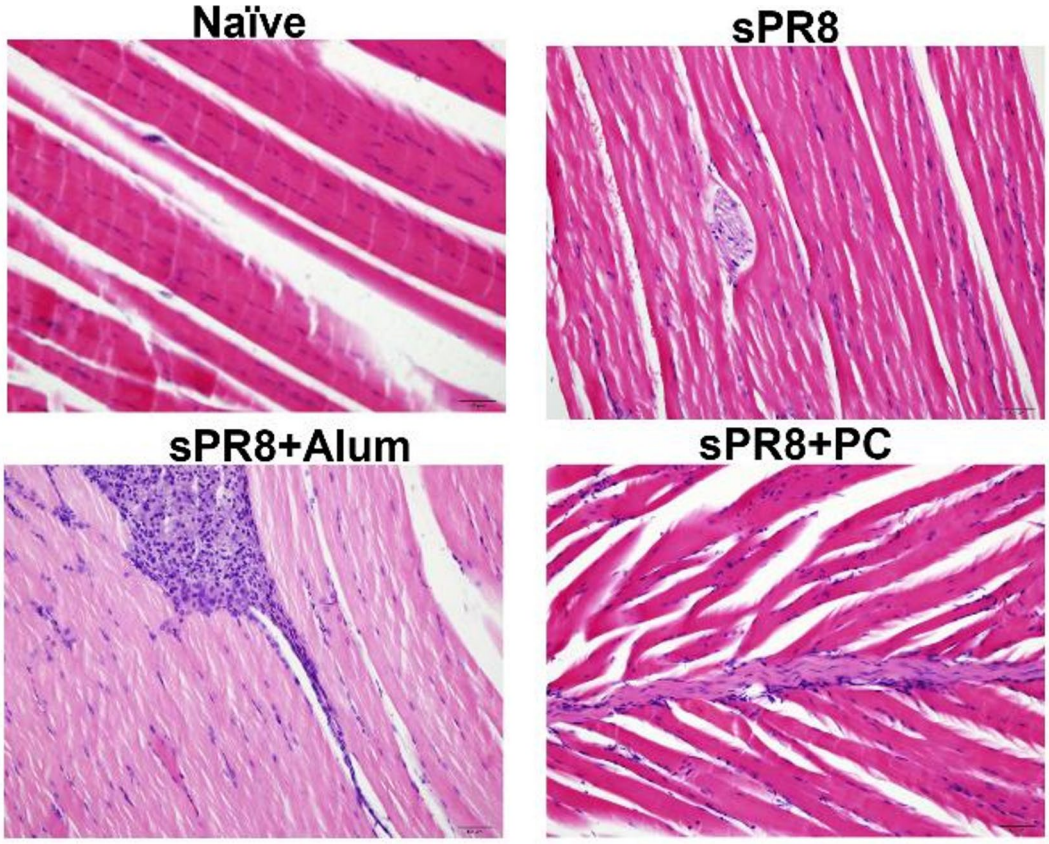

Fig. 7. Inflammation induced by the vaccination at the site of injection. Mice ($n = 3$/group) were given different vaccine regimens through intramuscular injections. Three days after the boost vaccination, the muscle tissues from the injection sites were collected, processed, and stained with H&E. The representative data are shown. Scale bars indicate 50 μm.

PC-adjuvant vaccine enhances immune responses via the TLR4 signaling pathway

Some marine algae extracts have been shown to induce the activation of TLR4 (Toll-like receptor 4) signaling[33,34]. Natural extracts containing polysaccharides have been shown to promote DC activation via the TLR4 pathway[35,36]. PC, a type of marine algae, also contains large amounts of polysaccharides[37,38]. Therefore, we conducted an in vitro experiment to evaluate whether PC enhances the immune response through the TLR4 pathway. BM-DCs were pre-treated for 1 h with 1 μM of TAK-242, a TLR4 pathway inhibitor. Then, BM-DCs were co-cultured for 2 days with either 0.1 μg/mL of MPL or various concentrations (4, 20, 100 μg/mL) of PC. The levels of CD40, CD86, and MHCII were analyzed by flow cytometry, and an ELISA was performed to measure the production of TNF-α, IL-6, IL-12p40, and IL-12p70. Increased levels of CD40 induced by either MPL or PC were significantly inhibited by TAK-242 (Fig. 8a). Furthermore, the enhanced production of TNF-α, IL-6, and IL-12p70, triggered by either MPL or PC, was markedly reduced by TAK-242 (Fig. 8b).

We investigated the ability of PC to induce TLR4 expression in vivo. Mice were administered either sPR8 (0.5 μg/mouse) alone, or in combination with PC (200 μg/mouse), or MPL (1 μg/mouse) during prime and boost vaccinations. Three days post-boost vaccination, we isolated proteins from the spleen and measured TLR4 expression using western blotting. MPL, a TLR4 ligand, was used as the positive control. According to the results, PC increased TLR4 expression, matching the levels observed with MPL; however, the difference was not significant (Fig. 8c, d). Overall, these findings suggest that PC stimulates BM-DC maturation and cytokine production via the TLR4 pathway.

Discussion

In recent years, there has been growing interest in the utilization and development of natural extracts as novel, safe, and efficacious vaccine adjuvants. The incorporation of adjuvants into vaccines is a strategy to improve vaccine-mediated protection, especially against influenza viruses. In this report, we investigated PC, an extract derived from marine algae, as a potential adjuvant in split influenza vaccines. In this research, we examined the effects of administering prime and boost vaccinations intramuscularly to mice and found promising results using PC as an adjuvant for influenza vaccines. We mainly assessed the impact of PC based on specific IgG1 and IgG2a serum antibodies, memory T and B cell responses, and protection against viral infections. Our findings indicate that the inclusion of PC significantly enhanced the efficacy of an inactivated split A/Puerto Rico/8/1934 H1N1 influenza vaccine (sPR8). When compared to sPR8 group, the vaccine with PC showed an improved

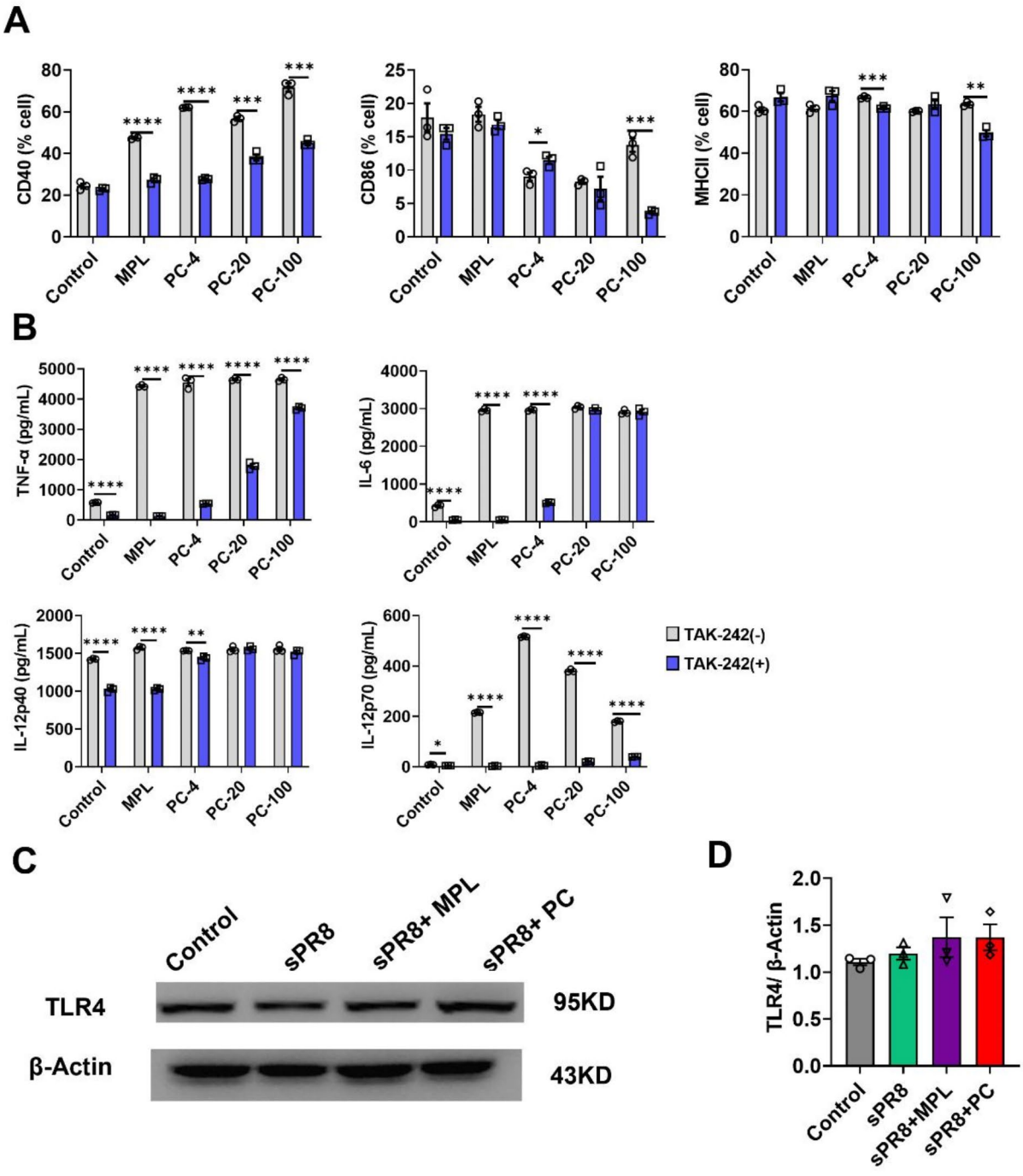

Fig. 8. TLR4 signaling pathway as a potential adjuvant mechanism of PC. (**a**, **b**) Effects of PC on BM-DCs function through the TLR4-mediated pathway were evaluated. After pre-treatment with 1 μM of TAK-242 for 1 h, BM-DCs were treated with different concentrations of PC (4, 20, 100 μg/mL) and 0.1 μg/mL MPL, incubated for 2 days. Activation marker expressions (**a**) and cytokine production (**b**) were then measured. (**c**, **d**) TLR4 expression levels in the spleen at day 3 post-boost vaccination were measured by western blot ($n = 3$). β-Actin was used as a loading control. Representative western blot images (**c**) and densitometry based quantitative analysis of TLR4 (**d**) are shown. Means ± standard error are shown with individual dots. One-way ANOVA and Tukey's multiple comparison test were performed for statistical analysis. $^{*}p < 0.0332$; $^{**}p < 0.0021$; $^{***}p < 0.0002$; $^{****}p < 0.0001$ compared between the indicated groups.

Th1/Th2 response and elicited significantly robust memory T and B cell reactions. Furthermore, mice that were administered PC exhibited better protection against severe infections, which was evident from the reduced lung inflammation, decreased viral loads, and prevention of weight loss caused by the viral infection.

The maturation and activation of DCs and macrophages not only play an important role in initiating antigen-specific immune responses, but also provide protective immunity against invading pathogens[39]. To understand the mechanism of PC-enhanced influenza vaccine-induced immunity, we investigated the maturation of DCs and macrophages in the muscle and ILN at the site of immunization 3 days post-boost vaccination. In this experiment, we selected MPL as a positive control due to its well-established role as a TLR4 agonist, known to effectively stimulate the activation of DCs and macrophages [40,41]. Our findings demonstrate that PC promotes the expression of CD40, CD86, and MHC II in DCs and macrophages in the ILN. Moreover, DCs activated by PC stimulated $CD4^+$ and $CD8^+$ T cell activation (Fig. 6e). These findings are consistent with those of our previous in vitro study[25], indicating that PC, as an adjuvant for the influenza vaccine, can improve immune responses by promoting DCs and macrophage maturation.

The effectiveness of an influenza vaccine is linked to its ability to stimulate both humoral- and cell-mediated immune responses. The humoral immune system produces antibodies to neutralize influenza antigens[42]. Our study found that using PC as an adjuvant enhanced the levels of antigen-specific IgG, IgG1, and IgG2a following both prime and boost vaccinations. The PC-adjuvant group showed elevated IgG2a levels compared to the alum group. Furthermore, consistent with prior reports on alum[43–45], our study showed its limited capability to induce IgG2a. Alum induces IgG1 but not IgG2a, highlighting its potential to initiate only a humoral immune response that correlates with the Th2-type immune response[46]. These data suggest that PC is a promising adjuvant for both cellular and humoral immunity. Cell-mediated immunity, primarily driven by T cells, including $CD4^+$ and $CD8^+$ T cells, has the potential to inhibit viral replication and expedite recovery following influenza virus infection[47]. In this study, we investigated the influence of PC-adjuvant vaccination on T cell proliferation. Our findings indicated that the PC-adjuvant vaccines notably enhanced the proliferation of antigen-stimulated $CD4^+$ and $CD8^+$ T cells, outperforming alum in both the lungs and spleen 2 weeks after boost immunization (Fig. 2). Moreover, 7 days after influenza virus infection, PC showed increased $CD4^+$ and $CD8^+$ T cell populations in both the spleen and lungs (Fig. 5a). These data suggest that PC-adjuvant vaccines have the potential to improve T cell immunity in split influenza vaccines. However, our data had limitations regarding antigen-specific T cell activation. Therefore, for further investigation, we plan to use tetramers to more thoroughly detect and identify antigen-specific $CD4^+$ and $CD8^+$ T cells, with particular attention to the potential for bystander activation.

Interestingly, we found differing patterns between the spleen and lungs in the memory T cell responses (Fig. 5a), which can be attributed to the distinct roles these organs play in the immune system and their involvement in local versus systemic immune responses. The lungs, as the primary site of infection in respiratory diseases like influenza, focused the immune response on local pathogen control [48,49]. This was demonstrated by the recruitment and activation of $CD4^+$ and $CD8^+$ T cells in the lungs, which were crucial for clearing the virus. Our data showed a relatively lower percentage of proliferating $CD4^+$ and $CD8^+$ T cells in the lungs compared to the spleen, likely because, by day 7 post-infection, the immune response in the lungs had begun to resolve. In contrast, the spleen, a key organ for systemic immune responses [50,51], exhibited a higher percentage of proliferating $CD4^+$ and $CD8^+$ T cells, reflecting its role in generating and maintaining memory immune cells that circulated throughout the body.

Cytokine storms and cell infiltration are key features of lung inflammation following influenza virus infection[28]. In the vaccinated group, we observed a significant reduction in inflammatory cytokine levels and cellular infiltration in the lungs on day 7 after a challenge with a lethal dose of the virus, compared to the naïve infected group, which had elevated levels (Fig. 4). Mice vaccinated with the PC adjuvant demonstrated significantly better control over viral replication upon infection compared to unvaccinated controls. This was evident in several key outcomes, including the prevention of weight loss (Fig. 3a, b), significantly reduced viral load in the lungs (Fig. 3d), and a marked decrease in cytokine secretion and inflammatory cell infiltration in the lungs (Fig. 4). This protective efficacy was not only superior to the non-immunized group but also highlighted the enhanced immune response provided by the PC adjuvant. The protective effects observed with the PC adjuvant are attributable to both humoral and cell-mediated immune responses. Specifically, the PC adjuvant induced elevated levels of antigen-specific IgG antibodies (Fig. 1), contributing to humoral immunity, and significantly enhanced the antigen-specific proliferation of $CD4^+$ and $CD8^+$ T cells (Figs. 2 and 5a), which play critical roles in cell-mediated immunity. Together, these immune mechanisms facilitated a more robust defense against the viral infection, demonstrating the PC adjuvant's potential as an effective component in vaccine formulations.

Alum is well known as a potent inducer of a Th2 immune response[52]. Interestingly, we observed a significantly increased number of eosinophils in the lungs of the alum-adjuvanted group at day 7 post-infection (Fig. 4). This can be attributed to alum's role in enhancing the Th2 response during vaccination, which leads to elevated eosinophil production and their migration to the site of antigen exposure, such as the lungs[53]. Furthermore, this eosinophilic response is a hallmark of a Th2-skewed immune reaction, aligning with the expected immunological outcome when alum is used as an adjuvant[54].

Innate immune cells are indispensable for the host defense against infectious pathogens[55,56]. This protective function is initiated when the immune system detects pathogen-associated molecular patterns through pathogen-recognition receptors (PRRs)[57,58]. These include toll-like receptors (TLRs), nod-like receptors, and RIG-I-like receptors (RLRs)[59]. Among these, TLRs are the most well-characterized class of PRRs[60,61]. Ligation of specific ligands to TLRs, particularly on antigen-presenting cells (APCs) such as dendritic cells, induces APCs activation[62]. This activation event triggers the release of pro-inflammatory cytokines and primes naïve T cells, setting the stage for the initiation of the adaptive immune response[63]. We assessed the enhancement of the immune response mediated by PC via the TLR4 signaling pathway. Our data indicate that PC enhanced the expression of the costimulatory molecules CD40 and CD86 on the surface of DCs (Fig. 8a). Furthermore, TLR4

signaling is known to skew towards Th1-type responses, typically characterized by increased production of IL-12p70 and IFN-α by APCs[64]. Consistent with this, our results demonstrated that PC treatment elevated IL-12p70 expression in DCs (Fig. 8a). Additionally, the expression of TLR4 in the spleen after boost vaccination in the PC-adjuvant group exhibited a higher level than the control group and showed the same level as the MPL-adjuvant group (Fig. 8b). This explains why PC-adjuvant mice showed heightened effectiveness in antigen-specific T cell responses induced by vaccination (Fig. 2).

We used alum as the positive control for the immunization and challenge studies but switched to MPL for the DC and macrophage activation experiments (Fig. 8) due to their distinct immunological pathways. Alum has been used more than 80 years with human vaccines as an adjuvant due to its immune-stimulatory and safety profile. It was used as a comparable control for the immunization in our study to evaluate adjuvant effects of PC in inducing general antigen-specific immune responses. However, it does not engage TLR4[65,66], making it not suitable for assessing TLR-associated mechanisms of PC. Since PC is thought to enhance immune responses via TLR4, we chose MPL, a well-known TLR4 agonist, as a control for the DC and macrophage activation. This switch allowed for a more accurate evaluation of PC's effects on TLR4-dependent immune responses, crucial for both innate and adaptive immunity. Our data show the PC-adjuvant vaccine enhanced immune responses via the TLR4 signaling pathway, and the activation of TLR4 effectively promoted both innate inflammatory responses and the induction of adaptive immunity. In this study, we utilized a total extract that likely contains multiple active compounds capable of engaging various PRR pathways, including TLR4. Although our primary focus was on the TLR4 pathway, we acknowledge that other PRRs may also be contributing to the observed immune response. In future studies, we plan to investigate the effects of the total PC extract and its individual compounds on distinct PRR pathways to better understand their specific impacts.

An ideal adjuvant should not only potentiate a targeted immune response, but also exhibit a safety profile characterized by minimal side effects[67]. Conventional adjuvants, such as Freund's Complete Adjuvant, QS21, and Quil A often show high inflammatory activity[68,69]. In the present study, we conducted toxicity assays in mice to evaluate the safety profile of PC. Throughout the experimental period, the mice exhibited no adverse behaviors, and there was no significant variation in body weight after vaccination (Supplementary Fig. 2). One objective of vaccine development is to minimize local inflammation at the injection site. Alum, MF59 (a squalene oil-in-water emulsion), and ASO4 (monophosphoryl lipid A and alum) have been employed as adjuvants in human vaccines; however, they can cause minor toxicities, leading to pain, redness, rash, swelling at the injection site, and even fever[70–72]. In this study, histological examination of the muscle containing the injection site revealed that the PC adjuvant elicited reduced inflammation at the injection site compared to the alum adjuvant (Fig. 7), corroborating findings from previous research[73,74]. These findings suggest that PC demonstrates a favorable safety profile as a potential adjuvant, serving as an initial step in evaluating its toxicity in vivo.

Our study reveals the potential of PC, a marine alga extract, as an effective adjuvant for split influenza vaccines. Our investigation underscores the ability of PC to enhance both humoral- and cell-mediated immune responses against influenza. Notably, PC not only augmented the activation of DCs and macrophages but also demonstrated a favorable safety profile in toxicity tests. Compared with traditional adjuvants, such as alum, PC exhibited reduced local inflammatory responses. Modulation of the TLR4 signaling pathway further illuminates the mechanism underlying the enhanced efficacy of PC, providing pivotal insights into its role in bolstering both innate and adaptive immune responses. In future studies, we plan to incorporate a TLR4 genetic knockdown model and investigate downstream signaling events, such as NF-κB activation, to gain a more comprehensive understanding of how PC interacts with TLR4 to enhance immune responses. Collectively, our findings indicate that PC is a promising adjuvant for the development of influenza vaccines.

Materials and methods

Animals

Female BALB/c and C57BL/6 mice (6–8 weeks old) were purchased from SamTako Bio Korea (Gyeonggi, Korea) and housed in an animal facility at the Jeju National University. All animal experiments were approved by the Institutional Animal Care and Use Committee of Jeju National University (protocol number: 2021-0051). All procedures involving animals were performed following the appropriate regulations and standards, and the reporting adhered to the ARRIVE guidelines.

Chemicals and reagents

An inactivated split A/PR8 vaccine (sPR8) was produced using the Influenza A virus strain A/Puerto Rico/8/1934 H1N1 [A/PR8]. The A/PR8 virus was first grown in the allantoic cavity of embryonated chicken eggs, next inactivated with 1% neutral formalin overnight at 4 °C, then concentrated by ultracentrifugation (30,000 round per minute (rpm), 1 h). The resulting inactivated virus pellet (iPR8) was resuspended in phosphate buffered saline (PBS) and treated with 1% Triton X-100 to break down the virus particles. After dialysis against PBS three times overnight to remove triton X-100 from the sPR8, the protein concentration of sPR8 was measured using the EZ-BCA protein quantification kit from DoGenBio (Seoul, Korea), and the vaccine was stored at -80 °C.

PC extract was provided by the Marine Biobank in Korea (Chungcheongnam-do, Korea, http://www.mabik.re.kr). Monophosphoryl lipid A (MPL) and alum were purchased from InvivoGen. All reagents were prepared according to the manufacturer's instructions.

Animal immunization and viral infection

BALB/c mice ($N = 8$/group) were intramuscularly injected with either the sPR8 vaccine alone (0.5 μg/mouse), or adjuvanted with alum (100 μg/mouse) or PC (200 μg/mouse) in 100 μL of PBS. The mice injected with PBS alone were used as controls. The immunization was administered twice—prime and boost—two weeks apart. Sera were collected 2 weeks after the prime vaccination and at 2, 4, 12, and 16-weeks post-boost. Sixteen weeks

after booster immunization, the mice were intranasally challenged with a lethal dose (1 × LD50) of the A/PR8 virus. Following infection, four mice from each group were monitored daily for 14 days to examine weight loss and survival rates. The other four mice were sacrificed 7 days post-challenge, and lung and spleen tissues were collected for subsequent experiments.

Memory B cell response assay

To investigate memory B cell and antibody-producing cell responses from the immunized mice, the cell culture plates were coated with 400 ng/well iPR8 overnight and blocked with 10% complete media (200 µL/well), which was RPMI media with 10% heat-inactivated fetal bovine serum (FBS) and 1% penicillin-streptomycin (Gibco), for 1 h at room temperature. The spleen and bone marrow cells from 7 days post-infection mice were harvested, seeded at a concentration of 2×10^6 cells/mL onto the plates, and incubated at 37 °C for 7 days and 1 day, respectively. Antigen-specific antibodies produced by the cells were detected using horseradish peroxidase (HRP)-labeled anti-mouse immunoglobulin IgG, IgG1, and IgG2a antibodies.

ELISA for antibody, cytokine, and chemokine levels

Two weeks after prime and boost immunizations, immune sera were collected, and the levels of antigen-specific antibodies were determined using ELISA. To perform the ELISA, inactivated A/PR8 virus (400 ng/well) was coated onto ELISA plates and then blocked using 1% bovine serum albumin and 0.05% TWEEN20 in PBS. The immune sera were serially diluted and added to ELISA plates, washed, and incubated with horseradish peroxidase-labeled secondary antibodies to detect antigen-specific IgG, IgG1, and IgG2a antibodies. Tetramethylbenzidine (TMB) was used as the substrate, and the optical density was measured at 450 nm using an ELISA reader.

To measure cytokine and chemokine in the lung extracts. Briefly, the lung tissues were homogenized in Roswell Park Memorial Institute (RPMI) 1640 medium (Fisher Scientific, Corning, NY, USA) using a 70 µm cell strainer, centrifuged at 1500 round per minute (rpm) for 5 min, and the resulting supernatant was collected for ELISA analysis. Interleukin (IL)-6, tumor necrosis factor (TNF)-α, IL-1β and IL-12p40 ELISA kits (Invitrogen, Waltham, MA) and Interferon (IFN)-γ, and CCL2 ELISA kits (R&D Systems, Minneapolis, MN) were used according to the manufacturer guidelines.

Lung viral titers

Sixteen weeks post-boost immunization, the mice were challenged with a lethal dose of the virus. Seven days after infection, lung tissues were collected from the challenged mice. These tissues were subsequently homogenized and centrifuged, and the resulting extracts were collected to assess the lung viral titer. The lung extracts were serially diluted and introduced into 10-day-old embryonated chicken eggs. Following an incubation period of 3 days, the allantoic fluid was harvested and examined for hemagglutination activity. The Reed and Muench method[75] was employed to calculate the concentration of infectious virus present in the lungs, expressed as the egg infectious dose 50 (EID50).

Evaluation of lung histopathology

For the histopathological analysis of the lung tissues after the lethal virus challenge, the left lower lobes were harvested from the mice at day 7 post infection. The tissue samples were preserved in 10% neutral buffered formalin, prepared, and then encased in paraffin. Thin sections of 1 µm were made and stained with Hematoxylin and Eosin (H&E). These lung sections underwent a blind evaluation, receiving scores between 0 and 4 for both peribronchial infiltrates and alveolar involvement. This assessment was based on a previously established histological scoring system[76].

Preparation of single cell suspension from tissues

The injected muscle tissues were processed and digested with Liberase TL as described in detail[77]. Briefly, skeletal muscle tissue from the site of vaccination was collected and digested with Liberase TL (0.25 mg/ml, Roche, Indianapolis, IN) plus DNase (0.25 mg/ml, Sigma Aldrich, St. Louis, MO) at 37 °C for 2 h under agitation, and Liberase activity was inactivated with complete media; RPMI media with 10% heat-inactivated FBS; and 1% penicillin-streptomycin (Gibco). Muscle digestions were filtered through 40 nm cell strainers (SPL Life Sciences, Korea), washed with FACs buffer, and prepared for staining for flow cytometry.

ILN, spleen, and lung tissues were cut by scissors and mechanically disrupted in 70 nm cell strainers using a plunger, centrifuged, and the pelleted cell blood was removed by ammonium-chloride-potassium (ACK) lysing buffer (Gibco) for 5 min at 4 °C. The cells were filtered through 40 nm cell strainers, washed, and stained.

DCs and macrophages activation in vivo

Cells from muscle and ILN were collected 3 days after boost vaccination with PBS (Control group), sPR8 (0.5 µg/mouse) alone, or in combination with PC (200 µg/mouse), or MPL (1 µg/mouse) through intramuscular injection. The mice were divided into four groups of three mice each. To analyze DCs and macrophage maturation, the cells were stained with CD11c-PE, CD11b-APC Cy7, MHC II-FITC, CD40-Qdot605, and CD86-APC. Stained cells were detected using FACs, and FlowJo (FlowJo, LLC, Ashland, OR) was used for data analysis.

The mixed lymphocyte reaction (MLR) assay

BALB/c mice ($n = 3$) were intramuscularly vaccinated with PBS (Control group), sPR8 (0.5 µg/mouse) alone, or in combination with PC (200 µg/mouse) or MPL (1 µg/mouse) through a prime-boost immunization regimen, with a 2-week interval between the prime and boost. Three days after the boost vaccination, dendritic cells (DCs) were isolated from the spleen using the EasySep™ Mouse Pan-DC Enrichment Kit II (STEMCELL Technologies, Canada) and co-cultured with CFSE-labeled naïve lymphocytes (LPC) from C57BL/6 mice. The lymphocytes

were first stained with carboxyfluorescein succinimidyl ester (CFSE), and the CFSE-labeled lymphocytes (10^6 cells/mL) were then co-cultured with DCs (10^5 cells/mL) in a 96-well U-bottom plate. After 5 days of incubation, the cells were harvested, and T-cell proliferation was evaluated using flow cytometry.

Inhibition experiments of TLR4 pathway

Immature DCs were prepared from bone marrow according to a previously reported method[78]. In brief, bone marrow from naïve BALB/c mice was isolated and cultured in RPMI-1640 medium containing 10% FBS, antibiotics, and 20 ng/mL of mouse granulocyte-macrophage colony-stimulating factor (mGM-CSF). After 6 days of culture, BM-DCs (1×10^6 cell/mL) were seeded in six-well plates (3 mL/well) and then treated with various concentrations of PC (4, 20, 100 μg/mL) for 12 h after the pre-treatment with 1 μM TAK-242 (TLR4 signaling inhibitor, CALBIOCHEM, Merck KGaA, Darmstadt, Germany) for 1 h at 37 °C. In the positive control, 0.1 μg/mL MPL was added. The expression levels of CD86, CD40, and MHC II were analyzed using flow cytometry. ELISA detected the yield of TNF-α, IL-6, IL-12p40, and IL-12p70.

Flow cytometry

Sixteen weeks post-boost immunization, the mice were challenged with a lethal virus. At day 7 post-infection, lung samples were collected to examine inflammatory cell infiltration. Single cells were extracted from lung samples and stained with specific antibodies for markers, including anti-mouse CD45 (clone 30-F11), anti-mouse F4/80 (clone BM8), anti-mouse MHC II (clone M5/114.15.2), anti-mouse CD11c (clone N418), anti-mouse CD11b (clone M1/70), anti-mouse CD170 (Siglec-F) (clone S17007L), anti-mouse Ly6c (clone AL-21) antibodies and LIVE/DEAD™ Fixable Aqua Dead Cell (Invitrogen™). First, lung cells were washed with FACs buffer (1x PBS contaning 2% FBS), and Fc receptors on their surfaces were blocked using anti-CD16/32 antibodies (Biosciences). Next, the antibody cocktail was added to the cells and incubated for 30 min at 4 °C. After washing, the stained cells were acquired using a High-end Performance Flow Cytometer, Beckman CytoFLEX, USA in the Bio-Health Materials Core Facility, Jeju National University. Data analysis was performed using FlowJo, and the phenotype of inflammatory cell infiltration in the lungs was determined using the gating strategies outlined in Supplementary Fig. S3.

Western blot analysis

Total proteins were isolated from spleen tissues 3 days post-boost vaccination using RIPA protein lysis buffer (Biosesang, Korea) mixed with Xpert Duo Inhibitor Cocktail solution (100:1; GeDEPOT, Korea). Three mice from each group were used for the western blot analysis.

The total protein concentration was quantified using the EZ-BCA protein quantification kit (DoGenBio, Seoul, Korea). The proteins were separated on 12% polyacrylamide-SDS gels and transferred onto PVDF membranes. Transferred membranes were blocked using 5% skim milk for 1 h at room temperature and then incubated at 4 °C overnight with anti-mouse TLR4 antibody (1:1,000, Santa Cruz, CA). The same membrane was probed with anti-β-actin (1:1,000; Santa Cruz, CA) as house-keeping protein. Next, the membranes were incubated with a horseradish peroxidase (HRP)-conjugated secondary antibody (1:5,000; Santa Cruz Biotechnology, Dallas, TX) at room temperature for 1 h after washing with TBST three times. Finally, the blots were developed using an EZ-Western Lumi Pico alpha kit (DoGenBio, Seoul, Korea).

Statistical analysis

Statistical analyses were performed using one-way or two-way ANOVA and Tukey's multiple comparison test at $P < 0.05$. All data are presented as means ± standard error with individual dots. GraphPad Prism software version 9.2.0 (GraphPad Software Inc., San Diego, CA) was used to analyze all data.

Data availability

The datasets used and/or analyzed during the current study available from the corresponding author on reasonable request.

Received: 6 March 2024; Accepted: 16 October 2024
Published online: 25 October 2024

References

1. Wang, B. & Loeb, M. in *Vaccinations* 89–103 (Elsevier 2019).
2. Iuliano, A. D. et al. Estimates of global seasonal influenza-associated respiratory mortality: a modelling study. *Lancet*. **391**, 1285–1300 (2018).
3. Kalil, A. C. & Thomas, P. G. Influenza virus-related critical illness: pathophysiology and epidemiology. *Crit. Care*. **23**, 1–7 (2019).
4. Taubenberger, J. K. & Morens, D. M. Influenza: the once and future pandemic. *Public Health Rep.* **125**, 15–26 (2010).
5. Kim, H., Webster, R. G. & Webby, R. J. Influenza virus: dealing with a drifting and shifting pathogen. *Viral Immunol.* **31**, 174–183 (2018).
6. Carter, D. & Reed, S. G. Role of adjuvants in modeling the immune response. *Curr. Opin. HIV AIDS*. **5**, 409 (2010).
7. Reyes, C. & Patarroyo, M. A. Adjuvants approved for human use: what do we know and what do we need to know for designing good adjuvants? *Eur. J. Pharmacol.* **945**, 175632 (2023).
8. Zhao, T. et al. Vaccine adjuvants: mechanisms and platforms. *Signal. Transduct. Target. Therapy*. **8**, 283 (2023).
9. Tregoning, J. S., Russell, R. F. & Kinnear, E. Adjuvanted influenza vaccines. *Hum. Vaccines Immunotherapeutics*. **14**, 550–564. https://doi.org/10.1080/21645515.2017.1415684 (2018).
10. Oleszycka, E. & Lavelle, E. C. Immunomodulatory properties of the vaccine adjuvant alum. *Curr. Opin. Immunol.* **28**, 1–5 (2014).
11. Didierlaurent, A. M. et al. AS04, an aluminum salt-and TLR4 agonist-based adjuvant system, induces a transient localized innate immune response leading to enhanced adaptive immunity. *J. Immunol.* **183**, 6186–6197 (2009).
12. Edelman, R. Vaccine adjuvants. *Rev. Infect. Dis.* **2**, 370–383 (1980).

13. Di Pasquale, A., Preiss, S., Tavares Da Silva, F. & Garçon, N. Vaccine adjuvants: from 1920 to 2015 and beyond. *Vaccines*. **3**, 320–343 (2015).
14. Nabel, G. J. Designing tomorrow's vaccines. *N. Engl. J. Med.* **368**, 551–560 (2013).
15. Coffman, R. L., Sher, A. & Seder, R. A. Vaccine adjuvants: putting innate immunity to work. *Immunity*. **33**, 492–503 (2010).
16. Dubensky, T. W. Jr & Reed, S. G. in *Seminars in immunology.* 155–161 (Elsevier).
17. Guiry, M. D. How many species of algae are there? *J. Phycol.* **48**, 1057–1063 (2012).
18. Cannell, R. J. Algae as a source of biologically active products. *Pest. Sci.* **39**, 147–153 (1993).
19. Manilal, A. et al. Antifouling potentials of seaweeds collected from the southwest coast of India. *World J. Agricultural Sci.* **6**, 243–248 (2010).
20. Hannan, M. A. et al. Neuroprotective potentials of marine algae and their bioactive metabolites: pharmacological insights and therapeutic advances. *Mar. Drugs*. **18**, 347 (2020).
21. Hwang, P. A., Lin, H. T. V., Lin, H. Y. & Lo, S. K. Dietary supplementation with low-molecular-weight fucoidan enhances innate and adaptive immune responses and protects against Mycoplasma pneumoniae antigen stimulation. *Mar. Drugs*. **17**, 175 (2019).
22. Jin, Y., Li, P. & Wang, F. β-glucans as potential immunoadjuvants: a review on the adjuvanticity, structure-activity relationship and receptor recognition properties. *Vaccine*. **36**, 5235–5244 (2018).
23. Sarei, F., Dounighi, N. M., Zolfagharian, H., Khaki, P. & Bidhendi, S. M. Alginate nanoparticles as a promising adjuvant and vaccine delivery system. *Indian J. Pharm. Sci.* **75**, 442 (2013).
24. Spolaore, P., Joannis-Cassan, C., Duran, E. & Isambert, A. Commercial applications of microalgae. *J. Biosci. Bioeng.* **101**, 87–96 (2006).
25. Ho, T. L. et al. Immunostimulatory effects of marine algae extracts on in vitro antigen-presenting cell activation and in vivo immune cell recruitment. *Food Sci. Nutr.* **11**, 6560 (2023).
26. Gao, R. et al. Cytokine and chemokine profiles in lung tissues from fatal cases of 2009 pandemic influenza A (H1N1): role of the host immune response in pathogenesis. *Am. J. Pathol.* **183**, 1258–1268 (2013).
27. Takano, T., Tajiri, H., Kashiwagi, Y., Kimura, S. & Kawashima, H. Cytokine and chemokine response in children with the 2009 pandemic influenza A (H1N1) virus infection. *Eur. J. Clin. Microbiol. Infect. Dis.* **30**, 117–120 (2011).
28. Liu, Q., Zhou, Y. & Yang, Z. -q. The cytokine storm of severe influenza and development of immunomodulatory therapy. *Cell Mol. Immunol.* **13**, 3–10 (2016).
29. Ryabkova, V. A., Churilov, L. P. & Shoenfeld, Y. Influenza infection, SARS, MERS and COVID-19: cytokine storm–the common denominator and the lessons to be learned. *Clin. Immunol.* **223**, 108652 (2021).
30. Chen, X. et al. Host immune response to influenza a virus infection. *Front. Immunol.* **9**, 320 (2018).
31. Mellman, I. Dendritic cells: master regulators of the immune response. *Cancer Immunol. Res.* **1**, 145–149 (2013).
32. Sheu, K. M. & Hoffmann, A. Functional hallmarks of healthy macrophage responses: their regulatory basis and disease relevance. *Annu. Rev. Immunol.* **40**, 295–321 (2022).
33. Fang, W. et al. Identification and activation of TLR4-mediated signalling pathways by alginate-derived guluronate oligosaccharide in RAW264. 7 macrophages. *Sci. Rep.* **7**, 1663 (2017).
34. Berri, M. et al. Ulvan from Ulva armoricana (Chlorophyta) activates the PI3K/Akt signalling pathway via TLR4 to induce intestinal cytokine production. *Algal Res.* **28**, 39–47 (2017).
35. Zhou, L. et al. Astragalus polysaccharides exerts immunomodulatory effects via TLR4-mediated MyD88-dependent signaling pathway in vitro and in vivo. *Sci. Rep.* **7**, 44822. https://doi.org/10.1038/srep44822 (2017).
36. Li, J. et al. Pleurotus ferulae water extract enhances the maturation and function of murine bone marrow-derived dendritic cells through TLR4 signaling pathway. *Vaccine*. **33**, 1923–1933 (2015).
37. Viola, R., Nyvall, P. & Pedersén, M. The unique features of starch metabolism in red algae. *Proc. R. Soc. Lond. B Biol. Sci.* **268**, 1417–1422 (2001).
38. Fritsch, F. E. *The Structure and Reproduction of the Algae Vol 2 Foreword, Phaeophyceae, Rhodophyceae, Myxophyceae* (Cambridge University Press, 1945).
39. Liu, J., Zhang, X., Cheng, Y. & Cao, X. Dendritic cell migration in inflammation and immunity. *Cell Mol. Immunol.* **18**, 2461–2471. https://doi.org/10.1038/s41423-021-00726-4 (2021).
40. Jeong, Y. et al. Dendritic cell activation by an E. coli-derived monophosphoryl lipid a enhances the efficacy of PD-1 blockade. *Cancer Lett.* **472**, 19–28 (2020).
41. De Becker, G. et al. The adjuvant monophosphoryl lipid A increases the function of antigen-presenting cells. *Int. Immunol.* **12**, 807–815 (2000).
42. Amanna, I. J., Carlson, N. E. & Slifka, M. K. Duration of humoral immunity to common viral and vaccine antigens. *N. Engl. J. Med.* **357**, 1903–1915 (2007).
43. Marrack, P., McKee, A. S. & Munks, M. W. Towards an understanding of the adjuvant action of aluminium. *Nat. Rev. Immunol.* **9**, 287–293 (2009).
44. Chen, X. et al. A novel laser vaccine adjuvant increases the motility of antigen presenting cells. *PLoS One*. **5**, e13776 (2010).
45. O'Hagan, D. T. & Singh, M. Microparticles as vaccine adjuvants and delivery systems. *Expert Rev. Vaccines*. **2**, 269–283 (2003).
46. Gupta, R. K. Aluminum compounds as vaccine adjuvants. *Adv. Drug Deliv. Rev.* **32**, 155–172 (1998).
47. Gianchecchi, E. et al. How to assess the effectiveness of nasal influenza vaccines? Role and measurement of sIgA in mucosal secretions. *Influenza Other Respir. Viruses*. **13**, 429–437 (2019).
48. Taubenberger, J. K. & Morens, D. M. The pathology of influenza virus infections. *Annu. Rev. Pathol. Mech. Dis.* **3**, 499–522 (2008).
49. Matrosovich, M. N., Matrosovich, T. Y., Gray, T., Roberts, N. A. & Klenk, H. D. Human and avian influenza viruses target different cell types in cultures of human airway epithelium. *Proceedings of the National Academy of Sciences* **101**, 4620–4624 (2004).
50. Bronte, V. & Pittet, M. J. The spleen in local and systemic regulation of immunity. *Immunity*. **39**, 806–818 (2013).
51. Mebius, R. E. & Kraal, G. Structure and function of the spleen. *Nat. Rev. Immunol.* **5**, 606–616 (2005).
52. HogenEsch, H. Mechanisms of stimulation of the immune response by aluminum adjuvants. *Vaccine*. **20**, S34–S39 (2002).
53. Kim, K. H. et al. Alum adjuvant enhances protection against respiratory syncytial virus but exacerbates pulmonary inflammation by modulating multiple innate and adaptive immune cells. *PloS One*. **10**, e0139916 (2015).
54. Chang, L. A. et al. Influenza breakthrough infection in vaccinated mice is characterized by non-pathological lung eosinophilia. *Front. Immunol.* **14**, 1217181 (2023).
55. Akira, S., Uematsu, S. & Takeuchi, O. Pathogen recognition and innate immunity. *Cell*. **124**, 783–801 (2006).
56. Kasuga, Y., Zhu, B., Jang, K. J. & Yoo, J. S. Innate immune sensing of coronavirus and viral evasion strategies. *Exp. Mol. Med.* **53**, 723–736 (2021).
57. Janeway, C. A. Jr & Medzhitov, R. Innate immune recognition. *Annu. Rev. Immunol.* **20**, 197–216 (2002).
58. Kumar, H., Kawai, T. & Akira, S. Toll-like receptors and innate immunity. *Biochem. Biophys. Res. Commun.* **388**, 621–625 (2009).
59. Li, D. & Wu, M. Pattern recognition receptors in health and diseases. *Signal. Transduct. Target. Therapy*. **6**, 291 (2021).
60. Duthie, M. S., Windish, H. P., Fox, C. B. & Reed, S. G. Use of defined TLR ligands as adjuvants within human vaccines. *Immunol. Rev.* **239**, 178–196 (2011).
61. Akira, S., Takeda, K. & Kaisho, T. Toll-like receptors: critical proteins linking innate and acquired immunity. *Nat. Immunol.* **2**, 675–680 (2001).
62. Kawasaki, T. & Kawai, T. Toll-like receptor signaling pathways. *Front. Immunol.* **5**, 461 (2014).
63. Iwasaki, A. & Medzhitov, R. Toll-like receptor control of the adaptive immune responses. *Nat. Immunol.* **5**, 987–995 (2004).

64. Jin, B., Sun, T., Yu, X. H., Yang, Y. X. & Yeo, A. E. The effects of TLR activation on T-cell development and differentiation. *Clinical and Developmental Immunology* (2012).
65. Eisenbarth, S. C., Colegio, O. R., O'Connor, W., Sutterwala, F. S. & Flavell, R. A. Crucial role for the Nalp3 inflammasome in the immunostimulatory properties of aluminium adjuvants. *Nature*. **453**, 1122–1126 (2008).
66. De Gregorio, E. & Rappuoli, R. From empiricism to rational design: a personal perspective of the evolution of vaccine development. *Nat. Rev. Immunol.* **14**, 505–514 (2014).
67. Pulendran, B., Arunachalam, S., O'Hagan, D. T. & P. & Emerging concepts in the science of vaccine adjuvants. *Nat. Rev. Drug Discovery*. **20**, 454–475. https://doi.org/10.1038/s41573-021-00163-y (2021).
68. Petrovsky, N. & Aguilar, J. C. Vaccine adjuvants: current state and future trends. *Immunol. Cell Biol.* **82**, 488–496 (2004).
69. Aguilar, J. & Rodriguez, E. Vaccine adjuvants revisited. *Vaccine*. **25**, 3752–3762 (2007).
70. Schwarz, T. F. et al. A ten-year study of immunogenicity and safety of the AS04-HPV-16/18 vaccine in adolescent girls aged 10–14 years. *Hum. Vaccines Immunotherapeutics*. **15**, 1970–1979 (2019).
71. Carmona, A. et al. Immunogenicity and safety of AS03-adjuvanted 2009 influenza a H1N1 vaccine in children 6–35 months. *Vaccine*. **28**, 5837–5844 (2010).
72. Harro, C. D. et al. Safety and immunogenicity trial in adult volunteers of a human papillomavirus 16 L1 virus-like particle vaccine. *J. Natl Cancer Inst.* **93**, 284–292 (2001).
73. Huntimer, L. et al. Evaluation of biocompatibility and administration site reactogenicity of polyanhydride-particle-based platform for vaccine delivery. *Adv. Healthc. Mater.* **2**, 369–378 (2013).
74. Zhang, W. et al. Comparison of PLA microparticles and alum as adjuvants for H5N1 influenza split vaccine: adjuvanticity evaluation and preliminary action mode analysis. *Pharm. Res.* **31**, 1015–1031 (2014).
75. Reed, L. J. & Muench, H. A simple method of estimating fifty per cent endpoints. *Am. J. Epidemiol.* **27**, 493–497 (1938).
76. Ahn, S. Y. et al. Chronic allergic asthma induces T-cell exhaustion and impairs virus clearance in mice. *Respir. Res.* **24**, 160. https://doi.org/10.1186/s12931-023-02448-9 (2023).
77. Liang, F. et al. Dissociation of skeletal muscle for flow cytometric characterization of immune cells in macaques. *J. Immunol. Methods*. **425**, 69–78 (2015).
78. Ko, E. J., Lee, Y. T., Lee, Y., Kim, K. H. & Kang, S. M. Distinct effects of Monophosphoryl lipid A, oligodeoxynucleotide CpG, and Combination adjuvants on modulating Innate and Adaptive Immune responses to Influenza Vaccination. *Immune Netw.* **17**, 326. https://doi.org/10.4110/in.2017.17.5.326 (2017).

Acknowledgements

This work was supported by a National Research Foundation of Korea (NRF) grant funded by the Korean government (MSIT) (RS-2023-00211504), the Basic Science Research Program to the Research Institute for Basic Sciences (RIBS) of Jeju National University through the NRF, funded by the Ministry of Education (2019R1A6A1A10072987) and Regional Innovation Strategy (RIS) through the National Research Foundation of Korea (NRF) funded by the Ministry of Education (MOE) (2023RIS-009).

Author contributions

Conceptualization and design: T.L.H., E.J.K.; Data generation and collection: T.L.H., S.Y.A.; Data Analysis: T.L.H., S.Y.A., E.J.K.; Data interpretation: T.L.H., S.Y.A., E.J.K.; Writing: T.L.H., E.J.K.; Review and editing: T.L.H., E.J.K.; Supervision: E.J.K.; All authors contributed significantly to the work, reviewed and finalized the manuscript.

Declarations

Competing interests

The authors declare no competing interests.

Additional information

Supplementary Information The online version contains supplementary material available at https://doi.org/10.1038/s41598-024-76736-9.

Correspondence and requests for materials should be addressed to E.-J.K.

Reprints and permissions information is available at www.nature.com/reprints.

Publisher's note Springer Nature remains neutral with regard to jurisdictional claims in published maps and institutional affiliations.

Open Access This article is licensed under a Creative Commons Attribution-NonCommercial-NoDerivatives 4.0 International License, which permits any non-commercial use, sharing, distribution and reproduction in any medium or format, as long as you give appropriate credit to the original author(s) and the source, provide a link to the Creative Commons licence, and indicate if you modified the licensed material. You do not have permission under this licence to share adapted material derived from this article or parts of it. The images or other third party material in this article are included in the article's Creative Commons licence, unless indicated otherwise in a credit line to the material. If material is not included in the article's Creative Commons licence and your intended use is not permitted by statutory regulation or exceeds the permitted use, you will need to obtain permission directly from the copyright holder. To view a copy of this licence, visit http://creativecommons.org/licenses/by-nc-nd/4.0/.

© The Author(s) 2024